NANO LETTERS

Letter

On the Microstructure of Nanoporous Gold: An X-ray Diffraction Study

Steven Van Petegem, Stefan Brandstetter, Robert Maass, Andrea M. Hodge, Bassem S. El-Dasher, Ju#rgen Biener, Bernd Schmitt, Camelia Borca, and Helena Van Swygenhoven

Nano Lett., **2009**, 9 (3), 1158-1163• DOI: 10.1021/nl803799q • Publication Date (Web): 04 February 2009

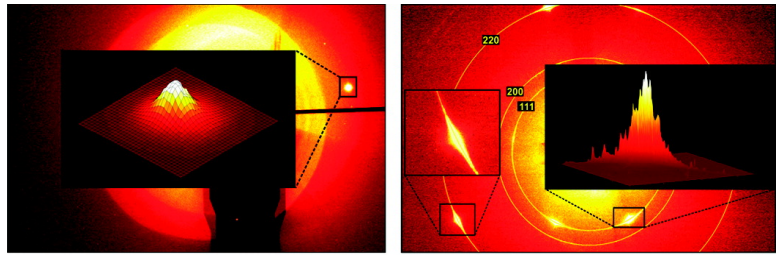

More About This Article

Additional resources and features associated with this article are available within the HTML version:

- Supporting Information
- Access to high resolution figures
- Links to articles and content related to this article
- Copyright permission to reproduce figures and/or text from this article

View the Full Text HTML

Nano Letters is published by the American Chemical Society. 1155 Sixteenth Street N.W., Washington, DC 20036

NANO LETTERS

2009
Vol. 9, No. 3
1158-1163

On the Microstructure of Nanoporous Gold: An X-ray Diffraction Study

Steven Van Petegem,[†] Stefan Brandstetter,[†] Robert Maass,[†] Andrea M. Hodge,[‡,§] Bassem S. El-Dasher,[‡] Jürgen Biener,[‡] Bernd Schmitt,[†] Camelia Borca,[†] and Helena Van Swygenhoven*[,†]

Paul Scherrer Institut, CH-5232 Villigen, Switzerland, and Nanoscale Synthesis and Characterization Laboratory, Lawrence Livermore National Laboratory, Livermore, California 94551-9900

Received December 16, 2008

ABSTRACT

The evolution of the grain structure, internal strain, and the lattice misorientations of nanoporous gold during dealloying of bulk (3D) Ag−Au alloy samples was studied by various in situ and ex situ X-ray diffraction techniques including powder and Laue diffraction. The experiments reveal that the dealloying process preserves the original crystallographic structure but leads to a small spread in orientations within individual grains. Initially, most grains develop in-plane tensile stresses, which are partly released during further dealloying. Simultaneously, the feature size of the developing nanoporous structure increases with increasing dealloying time. Finally, microdiffraction experiments on dealloyed micron-sized nanoporous pillars reveal significant surface damage introduced by focused ion beam milling.

Recently, nanoporous gold (np-Au) has attracted considerable attention fueled by its interesting mechanical properties[1,2] and its possible use in actuator,[3] sensor,[4−6] and catalysis[7] applications. The material can be easily prepared from Ag−Au alloys of suitable composition (e.g., $Au_{0.3}Ag_{0.7}$) by using a simple dealloying process and exhibits a characteristic spongelike structure with a unimodal pore size distribution on the nanometer length scale.[8−10] Although large progress has been made in understanding the fundamentals of the dealloying process,[8,11−13] there are still aspects that need to be addressed such as what happens to the microstructure of np-Au during dealloying. Current models assume that dealloying can be described by simple dissolution and diffusion processes on a rigid lattice without considering phenomena such as recrystallization or stress induced plastic deformation.[8] However, the observation that dealloying of Ag−Au alloys can lead to macroscopic sample shrinkage of up to 30% clearly demonstrates that plastic deformation during dealloying needs to be considered.[14] Indeed, surface stress-induced yielding of Au nanowires with diameters of a few nanometer (which most likely are being formed as intermediates during dealloying[12]) has been observed in atomistic simulations.[15] This immediately raises the question if, and to what extent, the microstructure of the Ag−Au starting alloy is preserved during dealloying, or if the grain structure is modified for example by stress-driven mechanical deformation. This is an important issue as changes in the microstructure can be expected to affect both the mechanical[16] and catalytic properties of nanoporous gold.[17−19] The existing experimental evidence is controversial. On one hand, dealloying experiments performed on ∼100 nm thin Ag−Au alloy films suggest that the crystal microstructure does not change dramatically during dealloying but also revealed the formation of strain inhomogeneities and/or defects.[9] On the other hand, transmission electron microscopy (TEM) micrographs of np-Au samples prepared from bulk (several hundred microns thick) samples of np-Au showed a nanocrystalline grain structure.[20] The question is whether these controversial results are real and reflect different experimental conditions (for example, two-dimensional (2D) versus three-dimensional (3D) samples), or are an artifact of the TEM sample preparation in case of 3D samples. For example, it is known that TEM sample preparation techniques such as microtome slicing and focused ion beam (FIB) milling can introduce surface relaxation and/or severe damage.[21,22] On the other hand, a 100 nm thick sample is certainly a more compliant substrate than a thick 3D sample, which should help to relieve the stresses developing at the dealloying front thus preventing plastic deformation to occur.

In this work, we addressed the questions raised above by performing time-resolved in situ X-ray diffraction experiments during dealloying of Ag−Au alloys followed up by a set of ex situ microstructural characterization experiments

* To whom correspondence should be addressed. E-mail: helena.vanswygenhoven@psi.ch.
[†] Paul Scherrer Institut.
[‡] Lawrence Livermore National Laboratory.
[§] Current address: Aerospace and Mechanical Engineering Department, University of Southern California, Los Angeles, California 90089.

10.1021/nl803799q CCC: $40.75
Published on Web 02/04/2009

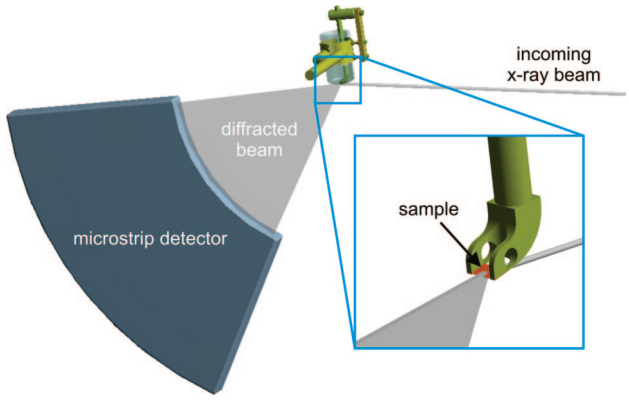

Figure 1. Schematic view of the in situ setup.

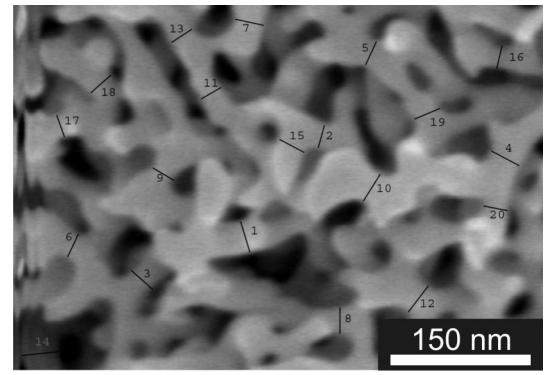

Figure 2. SEM image of the final nanoporous structure.

including X-ray microdiffraction. X-ray diffraction has the advantage of being a nondestructive technique capable of providing detailed information about the microstructure of 3D samples including grain size, lattice constant, and strains. Previous in situ X-ray diffraction studies on dealloying provided crucial information on the early stages of the dealloying process[23−25] but did not address the formation of the 3D nanoporous structure. In this study, we focus on the evolving microstructure in particular addressing the evolving internal stresses during dealloying and the lattice misorientations previously observed in TEM.

A polycrystalline $Au_{30}Ag_{70}$ alloy ingot was prepared by melting Au (99.999%) and Ag (99.999%) at 1100 °C and homogenizing the material for 70 h at 875 °C under an argon atmosphere. For the X-ray measurements ~50 μm thin strips were cut, polished, and then heat-treated for 8 h at 800 °C to relieve stress. The in situ X-ray experiments were performed at the powder diffraction station of the Materials Science beamline at the Swiss Light Source (SLS) in Switzerland. Figure 1 shows a schematic view of the setup. The Ag−Au samples with a thickness of about 50 μm are positioned in an Al sample holder and immersed in nitric acid in a standard Pyrex container. The bottom of the container is thinned to a thickness of 100 μm in order to reduce the background scattering arising from the amorphous Pyrex structure. In order to avoid tensile stress build up during dealloying because of sample shrinkage (see, e.g., refs 14 and 26), the samples are allowed to move in lateral direction. The incoming X-ray beam had a size of approximately 500 × 500 μm^2. In order to penetrate both the dissolving liquid and the specimen, an X-ray energy of 30 keV was chosen. The diffracted beam is recorded in reflection mode by the Mythen microstrip detector. The current version of this detector allows recording a full 120° X-ray diffraction pattern in a few seconds with negligible readout time. Note that in this geometry the angle between the incoming beam and the sample is fixed during the experiment.[27]

The in situ experiments are complemented by conventional X-ray diffraction, X-ray microdiffraction, and microscopy observations. The conventional X-ray measurements were performed in Bragg−Brentano geometry on a Siemens D500 laboratory diffractometer equipped with a Cu anode. The microdiffraction experiments were performed at the MicroXAS beamline of the Swiss Light Source. Here, the X-ray beam was focused to a size of 4 × 3 and 1 × 1 μm^2 for monochromatic (11.5 keV) and polychromatic (5−23 keV) light, respectively. The diffracted signal is recorded by a large 2D charge-coupled device detector in transmission geometry. For the Laue patterns, the diffraction peaks were identified with an automatic indexation routine using an approach similar as described in ref 28. The setup was calibrated using a strain-free Si wafer. The corresponding Laue diffraction pattern is shown in Supporting Information, Figure S1. The positions of the diffraction spots in a Laue pattern can be used to determine the local crystallographic orientation, similar to EBSD but with a much better resolution. Collecting Laue diffraction patterns at several positions within a single grain therefore allows one to identify rotational components.

Several in situ experiments were performed during which $Au_{30}Ag_{70}$ samples were immersed in nitric acid for several hours (free corrosion). Morphology (ligament size) and composition (amount of residual Ag) were assessed by cross-sectional scanning electron microscopy (SEM) and energy dispersive spectroscopy (EDAX). The SEM micrograph shown in Figure 2 was collected from a sample which was dealloyed for 4 h and reveals the formation of a nanoporous microstructure with an average ligament size of 31 ± 5 nm. The concentration of residual Ag in this sample was found to be less than 1% throughout the cross section indicating that the dealloying process was completed.

Electron backscatter diffraction (EBSD) inverse pole figure maps collected from the same sample area before and after dealloying are displayed in Figure 3. The $Au_{30}Ag_{70}$ alloy exhibits a broad grain size distribution with grain sizes ranging from a few tens up to several hundreds of micrometers. Furthermore the alloy does not exhibit strong texture. Note that the EBSD inverse pole figure maps suggest that both grain morphology and orientation are preserved during the dealloying process. On the other hand, cross-sectional TEM micrographs collected from the same area (using a FIB lit-out technique) indicted the formation of a textured nanocrystalline microstructure similar to that reported from microtomed cross sections of np-Au.[20] As we will show in the following, the observation of a nanocrystalline grain structure in cross sectional TEM samples seems to be an artifact of the TEM sample preparation.

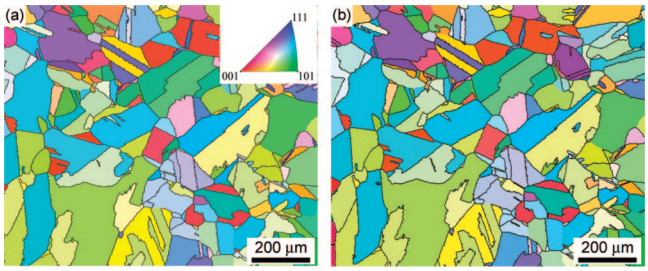

Figure 3. Electron backscatter diffraction (EBSD) inverse pole figure maps (1100 × 900 μm^2, step size was 2.5 μm) showing the grain structure and orientation (a) before and (b) after dealloying.

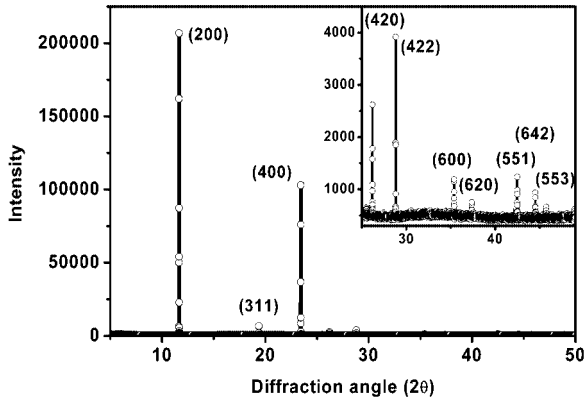

Figure 4. X-ray diffraction pattern of a $Au_{30}Ag_{70}$ sample before dealloying. The pattern for diffraction angles between 25 and 50° is shown in more detail in the inset.

Figure 4 displays a typical X-ray diffraction pattern of the initial $Au_{30}Ag_{70}$ alloy recorded with the in situ setup. Only a few diffraction peaks with high intensity can be observed. This is not due to the presence of texture but rather is a result of the large grain size in combination with a relatively small X-ray beam size, leading to a limited number of illuminated grains. This is illustrated in Supporting Information, Figure S2, which shows 4 diffraction patterns for which the angle between incoming X-ray beam and the sample was varied in steps of 0.2°. The large intensity variations between these spectra are typical for samples with grain sizes of the order of the size of the X-ray beam. For all in situ experiments this angle was chosen such that the spectrum contained at least three diffraction peaks with reasonable intensity. The diffraction peaks did not exhibit any size and/or strain broadening indicating a relaxed large-grained microstructure of our Ag−Au starting alloy.

The evolution of the (311) diffraction peak as function of dealloying time is shown in Figure 5. After a few minutes a very broad peak appears under the original narrow peak. This broad feature can be attributed to the formation of np-Au. Its intensity continuously increases at the expense of the intensity of the narrow diffraction peak. After about 30 min, the original diffraction peak has completely disappeared and only the contribution of nanoporous gold is left. A qualitative similar behavior is observed for the other diffraction peaks. Furthermore, no new diffraction peaks appear during dealloying. This observation reveals that the original microstructure is retained, consistent with the EBSD result shown in Figure 3.

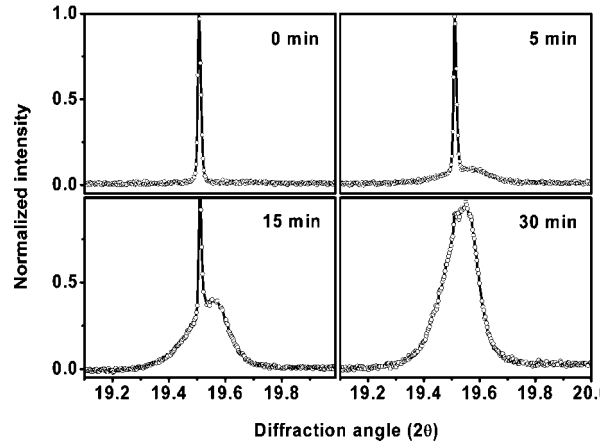

Figure 5. The (311) diffraction peak as function of dealloying time. The maximum intensity is normalized to 1.

The diffraction peaks were fitted with a split PearsonVII function. The evolution of the full-width at half-maximum (fwhm) of the broad component of the (311) and (400) diffraction peaks is displayed in Figure 6. A smooth decrease of the fwhm during dealloying is observed. This decrease is similar for all diffraction peaks and extends far beyond the completion of the Ag dissolution of this particular grain thus indicating that the feature size in np-Au increases continuously with time while being in contact with nitric acid. This coarsening is confirmed by SEM micrographs collected from a specimen that was dealloyed for only 0.5 h which leads to an average ligament size of ∼15 nm. Similar observations have also been reported by Newman and Sieradzki using in situ small-angle neutron scattering.[12] The coarsening of np-Au can be explained by curvature-driven surface diffusion which is assisted by the high mobility of gold atoms at the liquid-gold interface.

A conventional ex situ X-ray spectrum of the dealloyed sample was recorded with a large beam size that covers the entire sample. Here all diffraction peaks are present. Using a conventional Williamson−Hall (WH) analysis method, we find a coherent scattering length of 30 nm (consistent with our SEM observation) and a root-mean-square strain of 0.09%. This relatively small strain value is consistent with the mechanical robustness of our material despite the general brittleness of np-Au.[29] A WH analysis to deconvolute coherent scattering length and rms-strain from the diffraction data obtained during dealloying does not provide reliable results as only a few diffraction peaks are available. However, assuming a fixed value of 0.09% for the rms-strain we can derive the coherent scattering length from single diffraction peaks. The results for the (311) diffraction peak are shown in Figure 6 where we find a increase of the coherent scattering length from 10 to 45 nm during 4 h dealloying. Also shown in Figure 6 is the lattice strain, derived from the peak position. Clearly for this reflection, the lattice strain decreases significant from −0.25 to −0.07%, questioning the validity of the previous assumption of a constant rms-strain. Note that the lattice strain is negative,

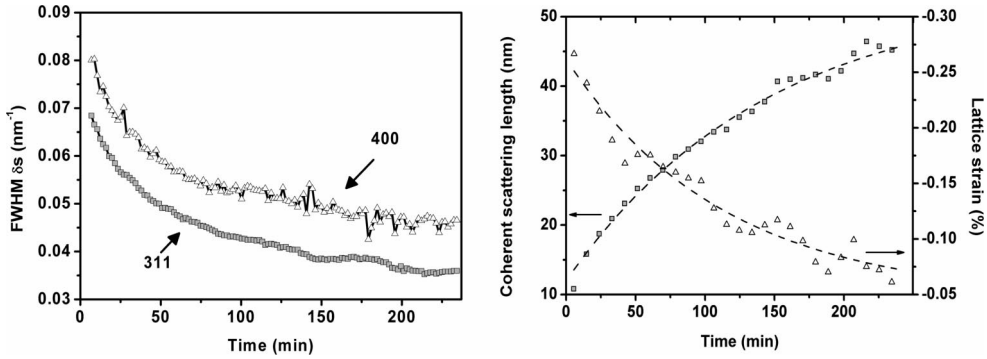

Figure 6. (left) Evolution of the fwhm of the (311) and (400) peak as function of dealloying time; (right) evolution of coherent scattering length and lattice strain as function of dealloying time as derived from the (311) diffraction peak.

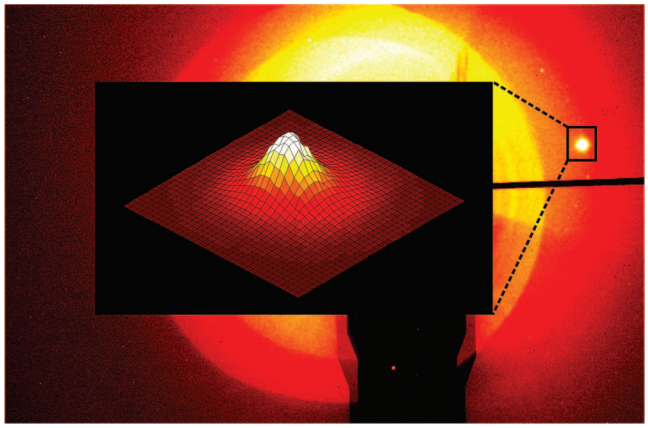

Figure 7. Typical two-dimensional microdiffraction pattern of nanoporous gold obtained with a monochromatic beam.

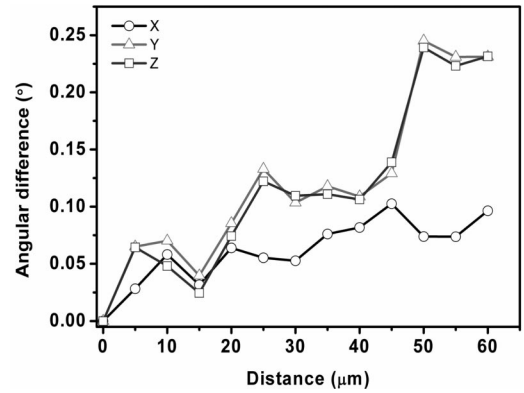

Figure 8. Relative change of the local crystal orientation within a grain. *Z* denotes the beam direction. *X* and *Y* are the horizontal and vertical in-plane directions, respectively.

which indicates compressive out-of-plane strain. It is worth pointing out that these results reflect microstructural changes in one or maybe a few grains only and may not be representative for the bulk behavior.

To obtain more detailed information about the microstructure of the ligaments X-ray microdiffraction experiments were performed on the samples after dealloying. Two-dimensional diffraction patterns are recorded with a micron-sized beam that is focused on a small volume within a single grain. Figure 7 displays a representative two-dimensional diffraction spectrum obtained with a monochromatic beam. It contains one high intensity broad diffraction spot with an approximately axisymmetric shape. For most grains, the positions of the diffraction spots reveal significant in-plane tensile strains. A few however are found to exhibit compressive strain.

Laue diffraction experiments were performed at various positions inside single grains, usually illuminating one or at most two grains. For all probed grains small but measurable lattice misorientations are observed. This is demonstrated in Figure 8 showing the angular change in crystallographic directions parallel and perpendicular to the beam direction during a line scan in a 70 μm grain. In this particular grain the crystal lattice mainly rotates around a direction parallel to the sample surface. Additionally, it was found that several grains are separated by $\Sigma 3$ boundaries (see, for instance-,Supporting Information, Figure S3).

The in and ex situ X-ray diffraction experiments reported here provide essential information on microstructural details of the nanoporous structure. The in situ X-ray measurements show that the microstructure of the original Ag−Au alloy is predominantly preserved, in contrast to our previous TEM observations. In particular, the development of new grain boundaries during dealloying was not observed as evidenced by the absence of rings (fully random granular structure) or parts of rings (textured structure) in our monochromatic X-ray microdiffraction experiments. In none of the probed grains could evidence for such a granular structure be found. On the contrary, all Laue diffraction patterns indicate the presence of at most two grains in the illuminated volume. However, we found evidence for small lattice misorientations within a grain (Figure 8). The preservation of the original grain structure results in a nonrelaxed microstructure with an rms-strain of about 0.1%, which is of the same order of magnitude as observed in some nanocrystalline materials with equivalent grain size. These rms-strains can originate from microstructural defects such as dislocations, or from inter- and intragranular stress variations.

In order to address in more detail the origin of the nanocrystalline structure reported after dealloying (ref 20), we investigated the influence of FIB damage on a nanoporous structure. Micron-sized pillars produced by FIB milling were investigated using microdiffraction. Pillars with a diameter of 4 μm and aspect ratio of 2.3 were produced by perpendicular FIB milling using a two-step procedure similar to

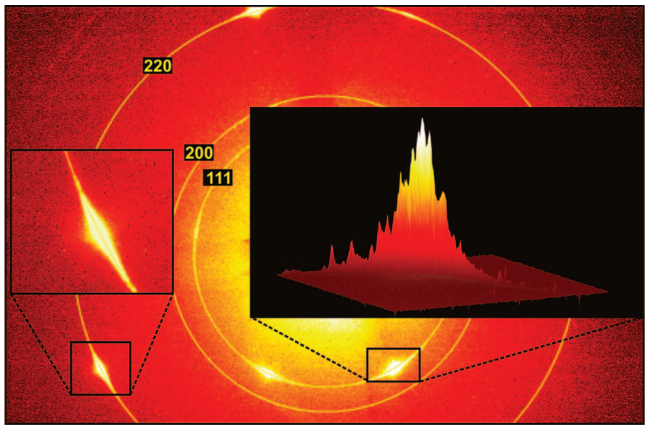

Figure 9. 2D X-ray microdiffraction image of a nanoporous gold pillar. The inset displays a 3D image of a part of the (111) ring.

the one described in refs 2 and 30. The pillars are positioned with micrometer precision in the X-ray beam using a fluorescence mapping technique.[31] The orientation of the pillars' vertical axes is determined to ~[2 3 9] by white beam Laue diffraction and the Laue patterns also disclose a (−1−11) twin contribution. Figure 9 displays a two-dimensional X-ray microdiffraction image taken with a monochromatic beam (11.5 keV) in the center of one of the pillars. Note the observation of several diffraction peaks in contrast to the typical microdiffraction pattern obtained from the original nanoporous structure (Figure 7). All peaks exhibit heavy azimuthal streaking indicating the presence of an orientation distribution of about 10−15 degrees on the indexed (111), (200), and (220) Debye rings. This is in agreement with the highly textured nanocrystalline structure observed in nanoporous TEM lamella produced by microtoming[20] or the FIB lift-out technique. Note that in this image the central part of the pillar, which is presumably not influenced by FIB damage and thus still single crystalline, is not in diffraction conditions and therefore not contributing to the diffraction pattern. The multiple ring segments, for instance on the (111) ring, presumably originate from the outer FIB damaged layer. The width of the diffraction peaks in radial direction is slightly narrower than expected, indicating possible ligament growth due to FIB milling, in agreement with observations by Sun and Balk.[21]

In conclusion, dealloying of bulk Ag−Au alloy samples by free corrosion results in the formation of a nanoporous structure that has a similar grain morphology and orientation as the original alloy sample. The grains exhibit a small spread in crystal orientation and often in-plane tensile stresses are observed, resulting in an rms strain of 0.1%. The presence of tensile stress is expected to negatively affect the mechanical robustness of this brittle material, and may also affect the catalytic properties of np-Au. Standard TEM sample preparation techniques such as microtoming and FIB lift-out were found to lead to severe plastic deformation resulting in an apparent nanocrystalline grain structure.

Acknowledgment. The authors thank D. Grolimund and M. Willimann from the MicroXAS beam line at the Swiss Light Source for technical support and C. A. Volkert for providing the nanoporous gold micropillars. H.V.S. thanks the Swiss National Science Foundation and the European Commission (6th Framework) for financial support of the project NANOMESO. Part of this work was performed under the auspices of the U.S. Department of Energy by Lawrence Livermore National Laboratory under contract DE-AC52-07NA27344.

Supporting Information Available: Figure S1: Laue pattern of a Si reference wafer with a ⟨001⟩ direction parallel to the beam direction and a ⟨110⟩ direction oriented along the vertical axis of the detector plane. Figure S2: diffraction patterns taken for increasing angles between sample and incoming X-ray beam. The angular difference between patterns A−D is 0.6°. Figure S3: a typical Laue diffraction pattern of bulk nanoporous gold after dealloying recorded with a micron-sized pink X-ray beam. This material is available free of charge via the Internet at http://pubs.acs.org.

References

(1) Biener, J.; Hodge, A. M.; Hayes, J. R.; Volkert, C. A.; Zepeda-Ruiz, L. A.; Hamza, A. V.; Abraham, F. F. *Nano Lett.* **2006**, *6*, 2379.
(2) Volkert, C. A.; Lilleodden, E. T.; Kramer, D.; Weissmuller, J. *Appl. Phys. Lett.* **2006**, *89*, 061920.
(3) Kramer, D.; Viswanath, R. N.; Weissmueller, J. *Nano Lett.* **2004**, *4*, 793–796.
(4) Biener, J.; Nyce, G. W.; Hodge, A. M.; Biener, M. M.; Hamza, A. V.; Maier, S. A. *Adv. Mater.* **2008**, *20*, 1211.
(5) Bonroy, K.; Friedt, J.-M.; Frederix, F.; Laureyn, W.; Langerock, S.; Campitelli, A.; Sara, M.; Borghs, G.; Goddeeris, B.; Declerck, P. *Anal. Chem.* **2004**, *76*, 4299–4306.
(6) Hieda, M.; Garcia, R.; Dixon, M.; Daniel, T.; Allara, D.; Chan, M. H. W. *Appl. Phys. Lett.* **2004**, *84*, 628–630.
(7) Zielasek, V.; Jurgens, B.; Schulz, C.; Biener, J.; Biener, M. M.; Hamza, A. V.; Baumer, M. *Angew. Chem., Int. Ed.* **2006**, *45*, 8241.
(8) Erlebacher, J.; Aziz, M. J.; Karma, A.; Dimitrov, N.; Sieradzki, K. *Nature* **2001**, *410*, 450.
(9) Roesner, H.; Parida, S.; Kramer, D.; Volkert, C. A.; Weissmueller, J. *Adv. Eng. Mater.* **2007**, *9*, 535.
(10) Fujita, T.; Qian, L. H.; Inoke, K.; Erlebacher, J.; Chen, M. W. *Appl. Phys. Lett.* **2008**, *92*, 251902.
(11) Erlebacher, J.; Sieradzki, K. *Scr. Mater.* **2003**, *49*, 991.
(12) Newman, R. C.; Sieradzki, K. *MRS Bull.* **1999**, *24*, 12.
(13) Erlebacher, J. *J. Electrochem. Soc.* **2004**, *151*, C614.
(14) Parida, S.; Kramer, D.; Volkert, C. A.; Rosner, H.; Erlebacher, J.; Weissmuller, J. *Phys. Rev. Lett.* **2006**, *97*, 035504.
(15) Diao, J. K.; Gall, K.; Dunn, M. L.; Zimmerman, J. A. *Acta Mater.* **2006**, *54*, 643.
(16) Hodge, A. M.; Biener, J.; Hsiung, L. L.; Wang, Y. M.; Hamza, A. V.; Satcher, J. H. *J. Mater. Res.* **2005**, *20*, 554.
(17) Mavrikakis, M.; Hammer, B.; Nørskov, J. K. *Phys. Rev. Lett.* **1998**, *81*, 2819.
(18) Gsell, M.; Jacob, P.; Menzel, D. *Science* **1998**, *280*, 717.
(19) Mavrikakis, M.; Stoltze, P.; Nørskov, J. K. *Catal. Lett.* **2000**, *64*, 101.
(20) Biener, J.; Hodge, A. M.; Hamza, A. V.; Hsiung, L. M.; Satcher, J. H. *J. Appl. Phys.* **2005**, *97*, 024301.
(21) Sun, Y.; Balk, T. J. *Scr. Mater.* **2008**, *58*, 727.
(22) Mayer, J.; Giannuzzi, L. A.; Kamino, T.; Michael, J. *MRS Bulletin* **2007**, *32*, 400.
(23) Renner, F. U.; Stierle, A.; Dosch, H.; Kolb, D. M.; Lee, T.-L.; Zegenhagen, J. *Nature* **2006**, *439*, 707.
(24) Renner, F. U.; Stierle, A.; Dosch, H.; Kolb, D. M.; Zegenhagen, J. *Electrochem. Commun.* **2007**, *9*, 1639.

(25) Renner, F. U.; Gründer, Y.; Lyman, P. F.; Zegenhagen, J. *Thin Solid Films* **2007**, *515*, 5574.
(26) Liu, Z.; Searson, P. C. *J. Phys. Chem. B* **2006**, *110*, 4318.
(27) Van Swygenhoven, H.; Schmitt, B.; Derlet, P. M.; Van Petegem, S.; Cervellino, A.; Budrovic, Z.; Brandstetter, S.; Bollhalder, A.; Schild, M. *Rev. Sci. Instrum.* **2006**, *77*, 013902.
(28) Tamura, N.; MacDowell, A. A.; Spolenak, R.; Valek, B. C.; Bravman, J. C.; Brown, W. L.; Celestre, R. S.; Padmore, H. A.; Batterman, B. W.; Patel, J. R. *J. Synchrotron Radiat.* **2003**, *10*, 137.
(29) Biener, J.; Hodge, A. M.; Hamza, A. V. *Appl. Phys. Lett.* **2005**, *87*, 121908.
(30) Volkert, C. A.; Lilleodden, E. T. *Philos. Mag.* **2006**, *86*, 5567.
(31) Maass, R.; Van Petegem, S.; Van Swygenhoven, H.; Derlet, P. M.; Volkert, C. A.; Grolimund, D. *Phys. Rev. Lett.* **2007**, *99*, 145505.

NL803799Q